Exploring mixed layer dynamics and light as limiting factors in the diatom community in the SJI

Ashlee Somol
Pelagic Ecosystem Function Research Apprenticeship Autumn 2023

Friday Harbor Laboratories, University of Washington, Friday Harbor, WA, 98250

asomol@uw.edu

Abstract

Stratification in the water column and its interplay with light has been historically observed to impact phytoplankton communities, most notably in Sverdrup's critical depth hypothesis. This study aims to examine stratification, light, and its relationship with marine diatoms within the San Juan Islands and contribute to the 20-year PEF dataset, and overall understanding of the oceanographic processes within the San Juan Islands. Phytoplankton net tows and CTD casts were conducted at two stations through the fall seasons to pinpoint the depth of the mixed layer and euphotic zone and characterize the marine diatoms present. Cells in the phytoplankton samples were counted and identified down to the genus level, and the diversity of the communities was calculated using the Shannon-Wiener diversity index. The mixed layer depth was found to be controlled by tidal action and much more variable at Station North (between 8-71 m) and winds at Station South (between 19-41 m). The euphotic zone had no correlation with these variables. Phytoplankton abundance and diversity were overall higher at Station South (max 3778 cells/L, 1.79 SWDI) than Station North (max 2855 cells/L, 1.17 SWDI). *Chaetoceros* was the most abundant genus at each station. After statistical analysis using 1-way ANOVA tests and pairwise correlation, no relationship was found between the mixed layer depth, the depth of the euphotic zone, and phytoplankton abundance and diversity. Instead, the abundance of phytoplankton was found to be primarily associated with PAR. Future studies could further look into the role of salinity and temperature impacting the phytoplankton, why *Chaetoceros* is overwhelmingly prolific, and studying drivers of phytoplankton diversity in the SJI.

Introduction

The mixed layer is a worldwide feature of the surface ocean that is characterized by a homogenous composition caused by turbulent mixing. This layer is directly influenced by the atmosphere as shear stress caused by winds and heat loss drive most of the mixing within the layer and separately, exchange gases across the air-surface interface (Giunta 2022). The energy, mass, and momentum of the mixed layer influence the movement and properties of the deep ocean (de Boyer 2004). Below the mixed layer, the deep ocean is not homogenous and can experience rapid changes in temperature, salinity, and density (Kantha 2002).

The depth of the mixed layer can vary greatly temporally and spatially. Solar radiation and lack of it heats and cools the surface of the ocean diurnally, creating variation on the scale of hours. Typically, the summer has the shallowest mixed layer depth (MLD) due to increased solar radiation heating the surface leading to stratification and the winter has the deepest MLD from stronger winds that cause mixing (Freeland 1997, Kara 2000, De Boyer 2004). In estuaries at mid-latitudes, the MLD is most heavily influenced by the salinity of the water and is shallower in comparison to polar regions where convection between the surface and the deep ocean causes a deeper MLD overall (Kantha 2002).

The fresher surface water and salty oceanic deep water of the estuary not only influence the MLD, they also create a unique environment for marine phytoplankton to thrive. Ebb and flood tides in the estuary which bring in more or less fresh water create fronts of opposing water masses where phytoplankton accumulate. These opposing fronts occur on flood tides, where the water column mixes and becomes more homogenous (Dustant 1989). The homogeny of the water column caused by mixing from flood tides decreases the depth of the mixed layer (Zhu 2020). When the mixed layer descends below a certain depth, the phytoplankton are unable to

bloom. This is known as the critical depth hypothesis, proposed by Sverdrup (1953), where the critical depth is defined as where the integrated photosynthesis above the depth is equal to the integrated respiration below. When the MLD shoals above the critical depth, it is possible for the phytoplankton to bloom.

Our study is focused on the San Juan Islands (SJI), a tide-dominated estuary, where freshwater intrusions at the surface from the nearby Fraser River further influence the MLD (Kantha 2002, MacCready 2020). Two stations were sampled over the fall season: Station North and Station South. Station North is located in a narrow, turbid channel between Yellow and San Juan Island, closer to the Fraser River input and reaching around 120 meters depth. Station South is located next to a glacial sill off San Juan Island into the Strait of Juan de Fuca, where there is strong water exchange in two-layer estuarine circulation with fresh Fraser River water at the surface and saline Pacific Ocean water below. These two stations have been sampled for the past 20 years for the Pelagic Ecosystem Function (PEF) apprenticeship, contributing to the overall oceanographic knowledge of the estuary. This study will further contribute to our understanding of the SJI by collecting and analyzing phytoplankton and chlorophyll samples from both stations throughout the Fall season.

Previous PEF apprentices have created a strong foundation of phytoplankton research in the region. Meredith Raith (2008) explored the relationship between phytoplankton abundance and tides and found that there are higher abundances during neap and slack tides. Ye Tian (2016) concluded that phytoplankton blooms occurred during periods of high water column stratification, which is contrary to Dustant et al. 1989 who concluded that phytoplankton were more abundant during flood tides, which mix the estuarine water column rather than stratify them. Zohreh Ramezanpour (2008) found that there was no correlation between phytoplankton

abundance and diversity and ebb versus flood tides. Contrary to Sverdrup's critical depth hypothesis, where a shoaled mixed layer creates conditions for phytoplankton to bloom, a study by Yoshie et al. 2002 shows that diatoms in the North Pacific benefit from a deeper mixed layer because it relieves the grazing pressure on the population by spreading the phytoplankton over a larger area.

This study aims to investigate the relationship between marine diatoms and the MLD within the SJI. Diversity and abundance data from phytoplankton samples taken around the islands as well as chlorophyll data taken aboard the R/V Kittiwake will be compared to the MLD both spatially and temporally. The data collected for this study will also be added and compared to the 20-year dataset collected by previous PEF students.

Methods

Phytoplankton Data

Starting in October 2023 in the San Juan Channel, six vertical phytoplankton tows were carried out at Station North (48.58° N, -123.05° W) and Station South (48.42° N, -122.95° W) aboard the R/V Kittiwake (Fig 1). The tows were completed on Oct 3rd, Oct 12th, Oct 17th, Oct 26th, Oct 31st, and Nov 7th using a phytoplankton net with an 80 μm mesh size and 8 cm radius lowered to 30 meters depth. The net was rinsed with seawater and the sample was preserved using a 2% formalin solution. The collected phytoplankton were then subsampled twice and mounted onto a Sedgewick-Rafter counting slides where cells were identified to the genus level and recorded until the 100th cell was counted. The average cell concentration was then calculated using the number of squares counted, where each square is equal to 1 μL.

Chlorophyll Data

Six CTD rosette casts using a Seabird CTD and 11 Niskin bottles were done at both

North and South stations. The CTD measured fluorescence as it ascended the water column. Water was subsampled in opaque dark 280 mL bottles from the Niskin bottles that were fired at 50 m, 20 m, 10 m (2 samples), and the surface (2 samples) and stored on ice until further processing. Upon returning to shore the water was then filtered using 25 mm GF/F and the filters sat in 10 mL of 90% acetone in a freezer overnight before being analyzed for chlorophyll and phaeopigments using a Turner 10-AU fluorometer.

Determining the Mixed Layer Depth and Euphotic Zone

For this study, the threshold method was used, where the reference depth was 0 m and the Δ sigma-t was 0.125 kg/m^3. Using the CTD data, the depth at which the potential density was 0.125 kg/m^3 more than the surface was determined to be the MLD.

A Secchi disk was used to determine the euphotic zone at all sampling sites. It was calculated using the Beer-Lambert Law rearranged into the following equation:

Eq. 1

$$z = -\frac{ln(\frac{Iz}{I0})}{k}$$

Where I_0 is the irradiance at the surface, I_z = 1% of I_0 and is the irradiance at the depth of the euphotic zone, k = 1.6/Secchi depth, and z is the depth of the euphotic zone. Irradiance data was taken from the Friday Harbor Labs Weather Station.

Statistical Analysis

To test for the significance of variables to the tides, one-way ANOVA tests were done in RStudio. Otherwise, all other tests were done using pairwise correlation plots in RStudio. The diversity of the phytoplankton community was determined using the Shannon-Wiener diversity index (SWDI) in the following equation:

Eq. 2

$$H = -\sum pi * ln(pi)$$

Where p_i is the relative abundance of the genus. Larger H values denote more diverse populations.

Results

Mixed Layer & Euphotic Zone Depth

The mixed layer depth at Station North was found to vary from depths as shallow as 8 meters to as deep as 71.5 meters (Fig. 2). The alternating pattern between shallow and deep mixed layers between cruise dates was of interest, so an exploration of possible factors was explored. An ANOVA test was run and found that deep mixed layers were associated with spring tides and shallow mixed layers were associated with neap tides ($p=0.01$) (Fig. 3). The highest MLDs were found at slack high tides and the lowest at slack low tides, though no significant correlation was found ($p=0.11$). This contrasts Station South, where the MLD was found to be between 41 and 19 meters. There was no CTD cast on the last cruise at Station South due to large waves. Further exploration into the Station South MLD incorporating a 24-hour time lag (Geary 1961) revealed that winds 24 hours prior to the sampling time were negatively correlated with the MLD (Fig. 4). Wind data for the day and time of the cruise as well as 24 hours prior was collected from NANOOS, using the NDBC New Dungeness buoy. The depth of the euphotic zone was the same at each station except for cruise 3, where the depth was 33.1 meters at Station North and 36.0 meters at Station South, and cruise 6, where the depth was 40.3 at Station North and 23.0 at Station South. The euphotic zone depth was not found to have any correlation with the MLD, tides, wind, or photosynthetically active radiation (PAR).

Chlorophyll

Chlorophyll amounts this year were much lower than in previous years. Further investigation into the specific instrument, calibration, and coefficients is ongoing but has not been finished by the end of this study. While discrete chlorophyll values seem incorrect, their values relative to each other align with phytoplankton samples. On October 12th, there was a major increase in chlorophyll values at Station South where it increased 0.08 µmol/L to 0.9 µmol/L (Fig. 5). The largest abundance of phytoplankton was recorded at Station South on this date from phytoplankton counts (Fig. 6). There is a similar increase in chlorophyll values at Station North on October 12th and October 17th where the three highest phytoplankton abundances were recorded (Fig. 5, Fig. 6). No chlorophyll sample was taken at Station South on October 17th at 50 meters depth and no CTD was cast for samples on November 7th.

Phytoplankton

A total of 12 phytoplankton samples were collected over the six cruises. Station North had a lower abundance on average than South, but had a higher abundance on the Oct 3rd cruise and Oct 17th cruise. The lowest abundance at Station North occurred on Oct 31st where there were 208 cells/L counted. Phytoplankton counts peaked on the Oct 17th cruise where there were 2855 cells/L counted rounded to the nearest whole number. Abundance overall at Station North increased from Oct 3rd to Oct 17th, and again from Oct 31st to Nov 7th (Fig. 6). Diversity decreased over the fall season, with a max SWDI of 1.17 on Oct 3rd and a minimum of 0.28 on Nov 7th (Fig. 6). The most abundant genus at North Station was *Chaetoceros*, accounting for an average of 87% of cells present throughout the whole season but peaking on Nov 7th at 95% of cells present. *Ditylum* and *Coscinodiscus* were also notable, at an average of 4.7% and 1.2% of cells present throughout the whole season. Despite being the second most abundant genus,

Ditylum steadily decreased throughout the season and was not found on the final cruise. Fifteen other genera were also present, making up less than 1% of the population each (Fig. 7).

Phytoplankton were overall more abundant at Station South and saw a peak at 3778 cells/L on Oct 12th. The lowest count was the day before on Oct 3rd at 205 cells/L. Abundance steadily decreased after the Oct 12th peak until Nov 7th, when there was an increase in abundance again, going from 786 cells/L to 1717 cells/L (Fig. 6). Diversity at Station South also decreased overall throughout the season but had a slight increase on Oct 31st going from 0.52 to 0.86 before decreasing to 0.09 on Nov 7th. The most abundant genus at Station South was also *Chaetoceros*, accounting for an average of 77% of the population throughout the Fall season. *Chaetoceros* accounted for 98% of the Nov 7th sample with *Coscinodiscus* and *Cylindotheca* being the only other genera present. Other notable genera found at Station South in order of abundance were *Coscinodiscus* at 5.7%*, Pseudo-nitzschia* at 4.5%*, Ditylum* at 2.8%*,* and *Skeletonema* at 1.7% (Fig. 8). Only two genera were not shared between both stations: *Eucampia* at North, and *Hemiaulus* at South.

Relationship between MLD, EZ, PAR, and Phytoplankton

There is no relationship or significant correlation between phytoplankton abundance and diversity with the depth of the mixed layer or the euphotic zone at either station. 1-way ANOVA tests also revealed no significant correlation between abundance and diversity with the tidal phase or current direction. Two periods of consistent sunny days were identified. Before the peak phytoplankton abundance on Oct 12th, there were 4 sunny days with PAR above 1100 μmol/m^2/s from Oct 5th through Oct 8th. Before the second increase in phytoplankton abundance at the end of the season, there were 6 sunny days with PAR above 900 μmol/m^2/s from Oct 26th through Oct 31st (Fig. 9). PAR steadily declined over the season. On a clear day, PAR reached close to

1300 μmol/m^2/s right before the start of the collection period (Sept 30th) whereas at the end of the season, a clear day would only reach around 940 μmol/m^2/s (Oct 30th) (Fig. 10). The diversity of phytoplankton showed a steady decline throughout the season along with daily average PAR (Fig. 11).

Discussion

There was no evidence of a relationship between the MLD, depth of the euphotic zone, and marine diatoms in the San Juan Archipelago (Fig. 12-15). Previous PEF researcher Ramezanpour explored the relationship between ebb and flood tides' impact on the marine phytoplankton community and concluded that there is no pattern of phytoplankton abundance and diversity except seasonal decline (2008). In contrast, the same year Raith found that chlorophyll-a concentrations had a strong correlation with slack tides, with the highest concentrations of chlorophyll-a occurring during slack tides (2008). This study collected samples on slack tides 6 of 12 times and found no relationship between slack tides and diatom abundance.

Tian speculated in 2016 that density stratification events coinciding with periods of high PAR would result in a Fall bloom citing at least 7 years between 2004 and 2016, though did not show how a stratification event was determined. The lack of relationship between MLD and phytoplankton in 2023 despite previous explorations of the matter could be explained through different interpretations of density, one being determined in this paper using the threshold method outlined in Monterey and Levitus (1997) and the other solely looking at Δ sigma-t between the surface and 20 meters depth.

This study contradicts previous research on the role of density stratification and the abundance of phytoplankton. In estuaries at latitudes around 40° during months of light-limited growth (November-January), density stratification can be the cause of temporal differences in

phytoplankton biomass (Sinclair 1981). Density stratification is not consistent throughout the whole estuary, instead more intense stratification is associated with the oceanic mouth of the estuary and a better-mixed water column is found closer to the river input where water is more turbid. Though there was a better-mixed water column at Station North, closer to the Fraser River, and a more stratified water column at Station South as you would expect to find, this stratification is associated with a higher abundance of phytoplankton that was not observed in this study.

Sinclair et al.1980 also concluded that tidal mixing is more important than wind mixing in shallow and fjord estuaries. While wind was found to be more important in mixing at Station South, the neap-spring tidal cycle was found to be the driving factor for mixing at Station North as predicted by Sinclair and observed in Puget Sound, another branch of the Salish Sea estuary. The tidal cycle has also been observed to affect phytoplankton biomass in other estuaries. A study in San Francisco Bay observed that phytoplankton blooms occur during the Spring season during neap tides. This is predicted by the critical depth hypothesis, as neap tides stratify the water column and trap phytoplankton within the euphotic zone and above the critical depth (1953). Lower rates of vertical mixing by tidal forces (5 m^2/day) coincide with a rapid increase in phytoplankton biomass and higher rates (50 m^2/day) are associated with low phytoplankton presence (Cloern 1991). This study agrees with neap-spring tide-driven mixing but additionally finds that neap tides are instead associated with a deeper mixed layer than a shallower one. This opposite effect to what has been observed and studied previously may relate to why there is no correlation between phytoplankton abundance in this study.

Instead, phytoplankton abundance is primarily correlated with PAR. Periods of sunny days preceded the two increases in abundance (Fig. 9). The highest phytoplankton count this year

had a period of four consistently sunny days before the cruise collection date. The sudden increase from less than 500 cells/L to over 3500 cells/L could be explained by the increase in PAR the community received. This trend has been observed by previous PEF researchers, most recently by Tian, who found that light was a controlling factor in the timing of blooms (2016). Raith also found that higher PAR coincided with higher concentrations of chlorophyll-a (2008). Light-limited growth in estuaries along similar latitudes has been recorded elsewhere as well as in Puget Sound (Sinclair 1981).

This study would benefit from nutrient data to support the assumption that growth in the San Juan Islands is not controlled by nutrients. Only the first two cruises had nutrient data available and showed nitrate and silicate presence far above limiting values. This limited data is supported by previous PEF observations of no nutrient depletion in the fall and winter seasons (Tian 2016, Ramezanpour 2008, Raith 2008). Other studies on phytoplankton growth in the Salish Sea found that estuarine nutrient circulation is saturated and not a limiting factor in phytoplankton growth (Li 2000, Belluz 2021).

There is competing evidence for the control of density on phytoplankton abundance from the PEF dataset, yet one thing remains constant: the dominance of *Chaetoceros*. Timothy Leung in 2018 synthesized data from 2004-2018 and found that *Chaetoceros* was the most abundant genus every year, except for in 2018 and 2022 when *Ditylum* dominated. Again, this year *Chaetoceros* was by far the most abundant phytoplankton present. Its relative abundance also increased steadily throughout the season as the diversity of phytoplankton decreased. *Chaetoceros* as a genus is regarded as one of the most abundant and diverse genus of marine diatoms (Malviya 2016, De Luca 2021). This cannot be the sole reason for its abundance, as similarly globally abundant genera of diatoms such as *Corethron* and *Thalassiosira* were only

seen on 4 of 6 cruises at a max of 0.9% of the population and 2 of 6 cruises at a max of 1.95% of the population respectively (Malviya 2016). *Chaetoceros* dominance during the fall season has also been recorded in other estuaries (Yang 2014, Rines 1987).

Previous research on *Chaetoceros* has incorporated temperature and light into their experiments and found that higher temperatures increase the growth rate of *C. calcitrans* (Kong 2021). Leung found in his synthesis of phytoplankton data that sea surface temperature has a significant impact on the diversity and abundance of marine diatoms. A deeper exploration of *Chaetoceros* abundance in relation to sea temperature and PAR may reveal the driving factor for its dominance in the SJI. Leung also observed a decrease in phytoplankton diversity through the period 2007-2018. More specifically, PEF research Phil Green in 2010 found a negative correlation between *Skeletonema* and *Chaetoceros* abundance and speculated that it was due to varying salinity throughout the season. The driving factors for the diversity of phytoplankton in the SJI could be explored in much more detail.

Acknowledgements

I thank the captain and crew of the R.V. Kittiwake and R.V. Rachel Carson for their patience and support. I thank my mentors Jan Newton, Alex Marquez, Becca Guenther, Matt Baker, and Mike Sigler for their knowledge, feedback, and guidance. I thank my fellow research apprentices for all their hard work on the boat and onshore in collecting and entering the data collected.

References

1. Belluz, J. D. B., et al. (2021). Phytoplankton Composition and Environmental Drivers in the Northern Strait of Georgia (Salish Sea), British Columbia, Canada. *Estuaries and Coasts*, *44*, 1419–1439 (2021). https://doi.org/10.1007/s12237-020-00858-2
2. Cloern, J. (1991). Tidal stirring and phytoplankton bloom dynamics in an estuary. *Journal of Marine Research. 49.* 203-221. 10.1357/002224091784968611.
3. Cloern, J. E. (1987). Turbidity as a control on phytoplankton biomass and productivity in estuaries. *Continental Shelf Research*, *7*(11-12), 1367-1381. https://doi.org/10.1016/0278-4343(87)90042-2
4. Diaz, B. P., et al. (2021). Seasonal mixed layer depth shapes phytoplankton physiology, viral production, and accumulation in the North Atlantic. *Nature Communications*, *12*(1), 1-16. https://doi.org/10.1038/s41467-021-26836-1
5. Dustan, P., et al. (1989). Tidally induced estuarine phytoplankton patchiness. *Limnology & Oceanography, 34*(2), 410-419. https://doi.org/10.4319/lo.1989.34.2.0410
6. Freeland, H., et al. (1997). Evidence of change in the winter mixed layer in the Northeast Pacific Ocean. *Deep Sea Research Part I: Oceanographic Research Papers*, *44*(12), 2117-2129. https://doi.org/10.1016/S0967-0637(97)00083-6
7. Giunta, V., & Ward, B. (2022). Ocean Mixed Layer Depth From Dissipation. *Journal of Geophysical Research: Oceans*, *127*(4), e2021JC017904. https://doi.org/10.1029/2021JC017904
8. Kantha, L., et al. (2002). Ocean mixed layer. *Encyclopedia of Atmospheric Sciences* (pp.8).

9. Kara, A. B., Rochford, P. A., & Hurlburt, H. E. (2000). Mixed layer depth variability and barrier layer formation over the North Pacific Ocean. *Journal of Geophysical Research: Oceans*, *105*(C7), 16783-16801. https://doi.org/10.1029/2000JC900071
10. Kong, F., et al. (2021). Synergistic effects of temperature and light intensity on growth and physiological performance in Chaetoceros calcitrans. *Aquaculture Reports*, *21*, 100805. https://doi.org/10.1016/j.aqrep.2021.100805
11. Leung, T. (2018). Temporal Variation of the Fall Phytoplankton Community at the San Juan Archipelago
12. Li, M., et al. (2000). What Determines Seasonal and Interannual Variability of Phytoplankton and Zooplankton in Strongly Estuarine Systems? *Estuarine, Coastal and Shelf Science*, *50*(4), 467-488. https://doi.org/10.1006/ecss.2000.0593
13. Lorbacher, K., Dommenget, D., Niiler, P. P., & Köhl, A. (2006). Ocean mixed layer depth: A subsurface proxy of ocean-atmosphere variability. *Journal of Geophysical Research: Oceans*, *111*(C7). https://doi.org/10.1029/2003JC002157
14. Luca, D., et al. (2019). Global distribution and diversity of Chaetoceros (Bacillariophyta, Mediophyceae): Integration of classical and novel strategies. *PeerJ*, *7*. https://doi.org/10.7717/peerj.7410
15. MacCready, P., et al. (2021). Estuarine Circulation, Mixing, and Residence Times in the Salish Sea. *Journal of Geophysical Research: Oceans*, *126*(2), e2020JC016738. https://doi.org/10.1029/2020JC016738
16. Malviya, S., et al. (2016). Insights into global diatom distribution and diversity in the world's ocean. *Proceedings of the National Academy of Sciences*, *113*(11), E1516-E1525. https://doi.org/10.1073/pnas.1509523113

17. Raith, M. (2008). Physical and biological processes affecting chlorophyll-a concentrations within the San Juan Archipelago in fall 2008
18. Ramezanpour, Z. (2008). Distribution and diversity of the phytoplankton community in San Juan Channel with respect to tide and other controlling factors
19. Rines, J. E., et al. (1987). The seasonal distribution of the marine diatom genus Chaetoceros Ehr. In Narragansett Bay, Rhode Island (1981–1982). *Journal of Plankton Research*, *9*(5), 917-933. https://doi.org/10.1093/plankt/9.5.917
20. Sinclair, M., et al. (1981). Phytoplankton temporal distributions in estuaries. *Oceanologica Acta, 4*(2), 239-246.
21. Sverdrup, H. U. (1953). On Conditions for the Vernal Blooming of Phytoplankton. *ICES Journal of Marine Science*, *18*(3), 287-295. https://doi.org/10.1093/icesjms/18.3.287
22. Talke, S. A., et al. (2010). Mixing layer dynamics in separated flow over an estuarine sill with variable stratification. *Journal of Geophysical Research: Oceans*, *115*(C9). https://doi.org/10.1029/2009JC005467
23. Tian, Y. (2016). Phytoplankton abundance, distribution, community composition and physical controls in San Juan Channel during Fall
24. Yang, S., et al. (2014). Seasonal changes in phytoplankton biomass and dominant species in the Changjiang River Estuary and adjacent seas: General trends based on field survey data 1959–2009. J. *Ocean Univ. China. 13*, 926–934. https://doi.org/10.1007/s11802-014-2515-7
25. Yoshie, N., et al. (2003). One Dimensional Ecosystem Model Simulation of the Effects of Vertical Dilution by the Winter Mixing on the Spring Diatom Bloom. *Journal of Oceanography, 59*, 563-571. https://doi.org/10.1007/s11802-014-2515-7

26. Zhu, L., et al. (2020). Response of Stratification Processes to Tidal Current Alteration due to Channel Narrowing and Deepening. *Journal of Geophysical Research: Oceans*, *125*(2), e2019JC015223. https://doi.org/10.1029/2019JC015223

Figures

Fig. 1

Figure 1. Generated using Geolocate (https://www.geo-locate.org/web/WebGeoref.aspx) Bing Aerial maps.

Fig. 2

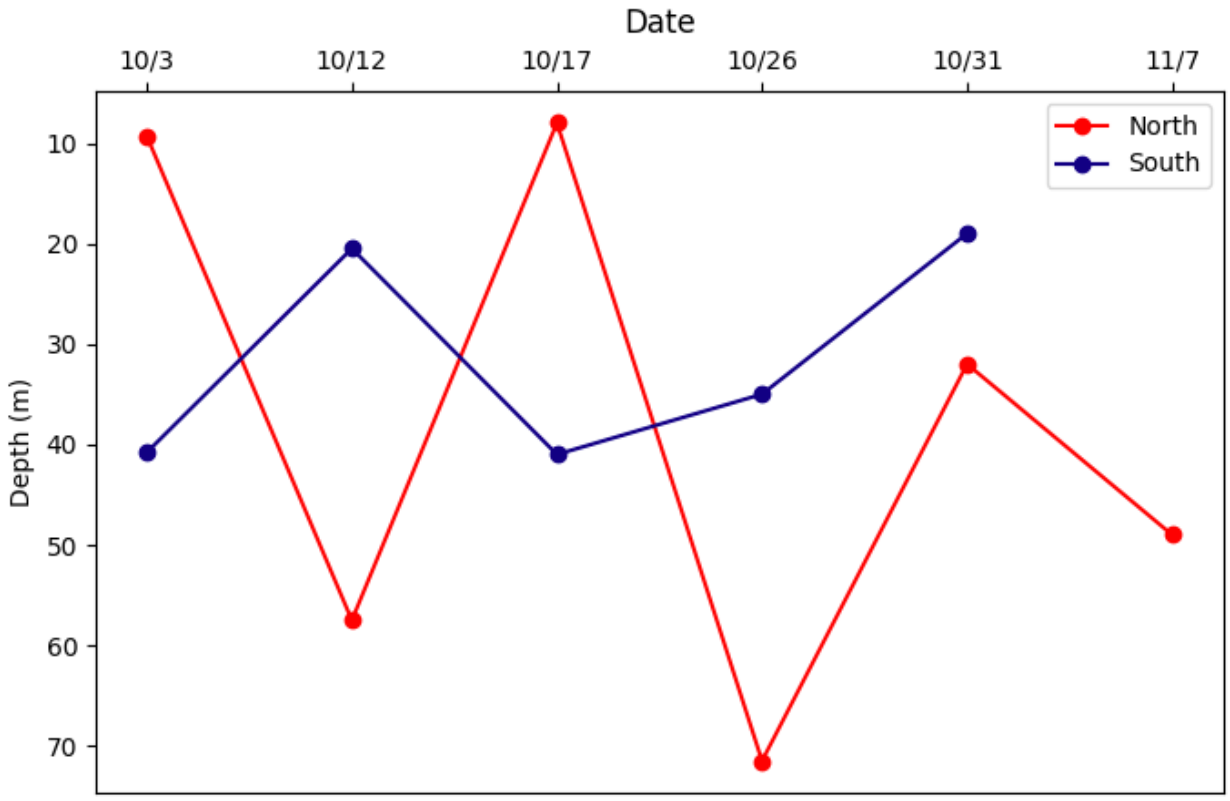

Figure 2. Fall 2023 time series of the mixed layer depth of Station North and Station South on cruise dates.

Fig. 3

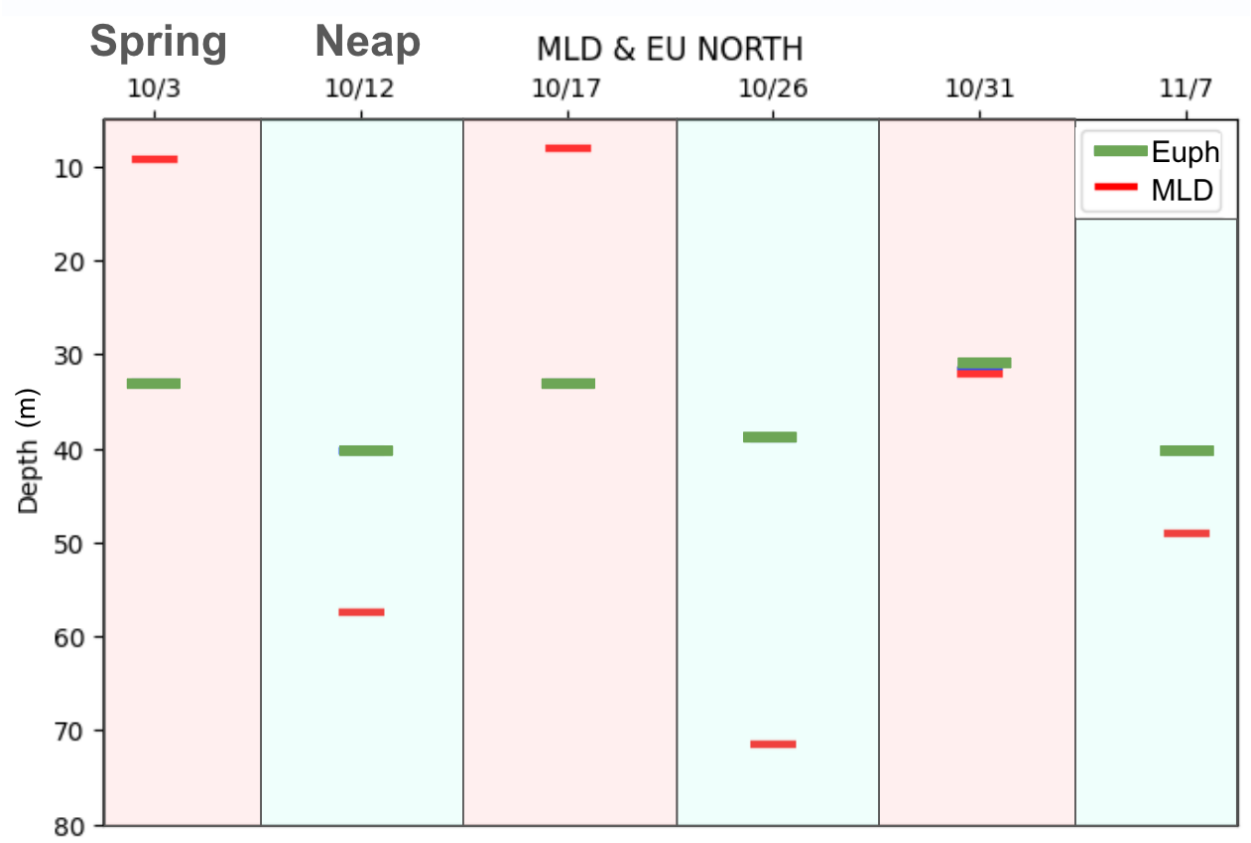

Figure 3. Fall 2023 time series of the MLD and depth of the euphotic zone with respect to the spring/neap tidal cycle. Red highlighted data points are during spring tides, and blue highlighted data points are during neap tides.

Fig. 4

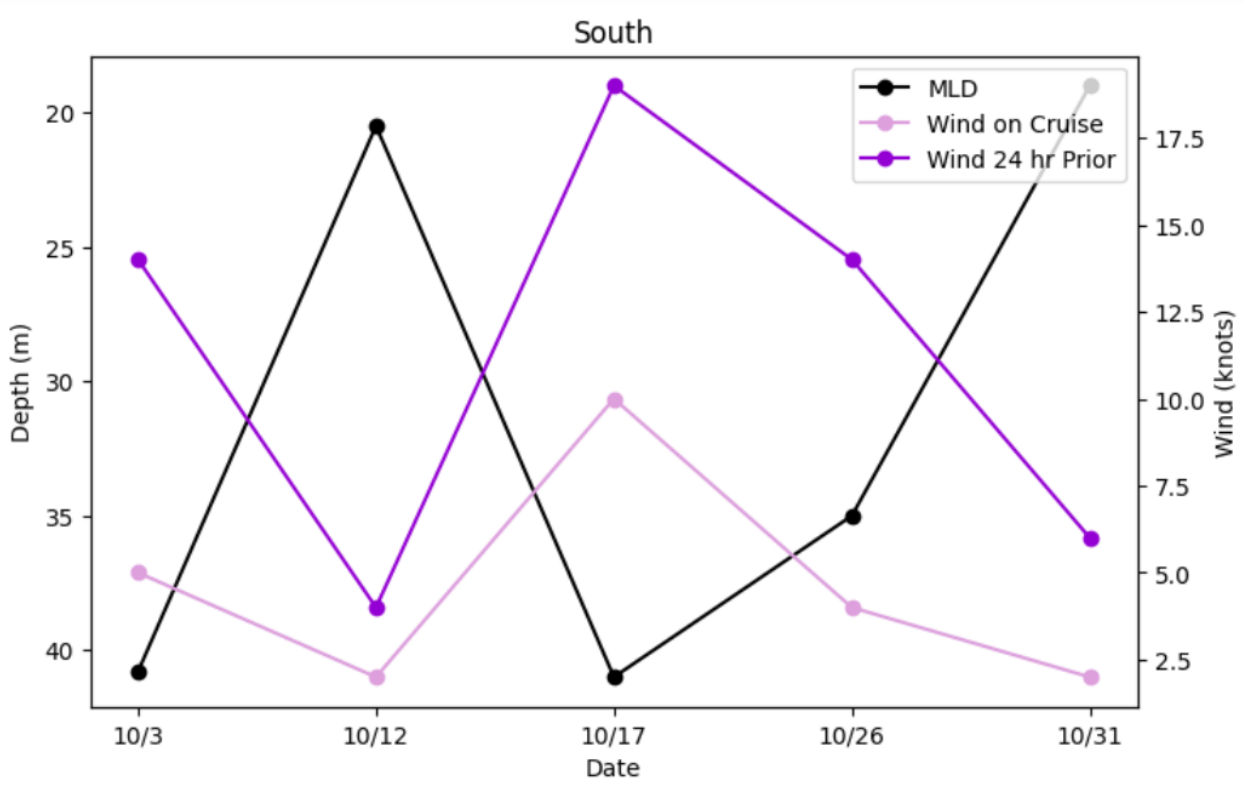

Figure 4. Fall 2023 time series of the mixed layer depth at Station South with wind data from the day and time of the cruise and 24 hours prior. Depth is inverse on the left axis and wind is on the right axis. Wind data found through NANOOS (https://www.nanoos.org/)

Fig 5.

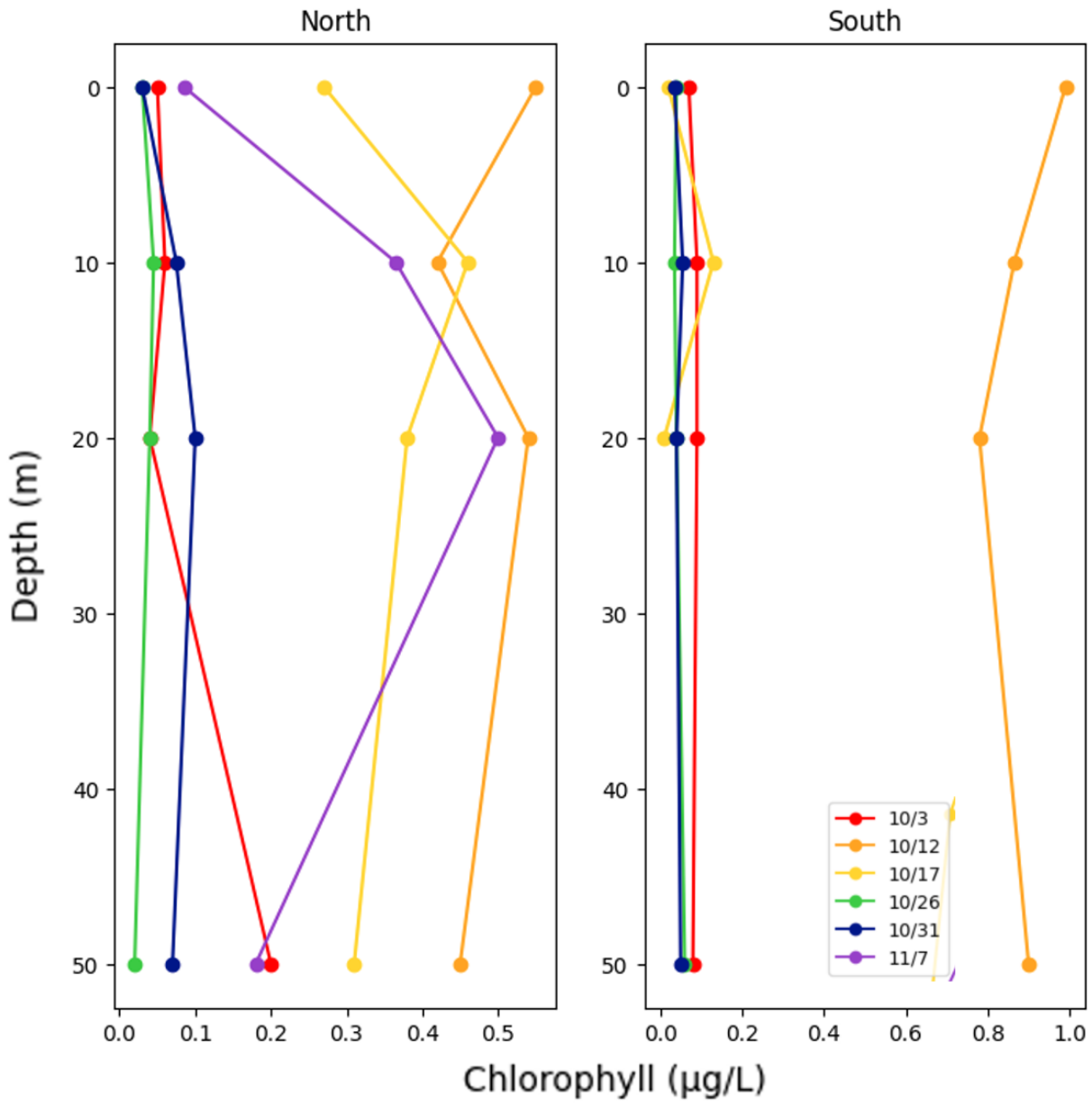

Figure 5. Chlorophyll samples with depth at North and South stations.

Fig. 6

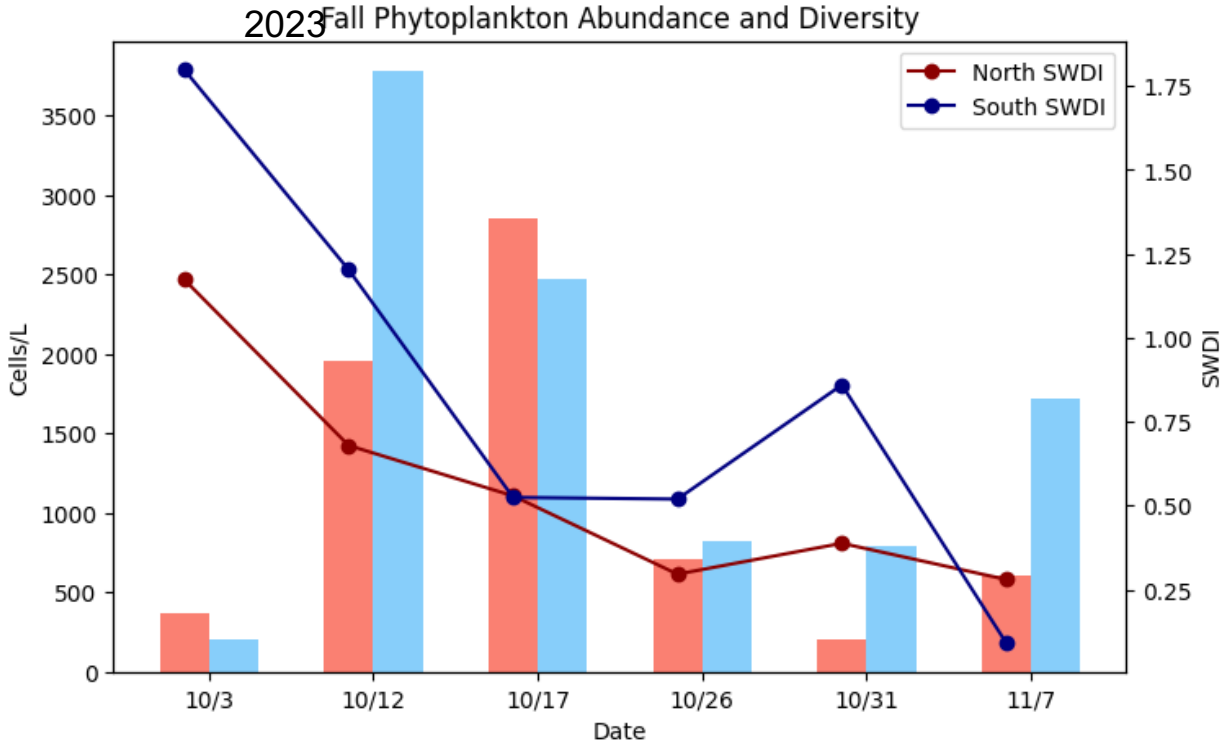

Figure 6. Fall 2023 time series of phytoplankton abundance on the left axis and diversity on the right axis.

Fig. 7

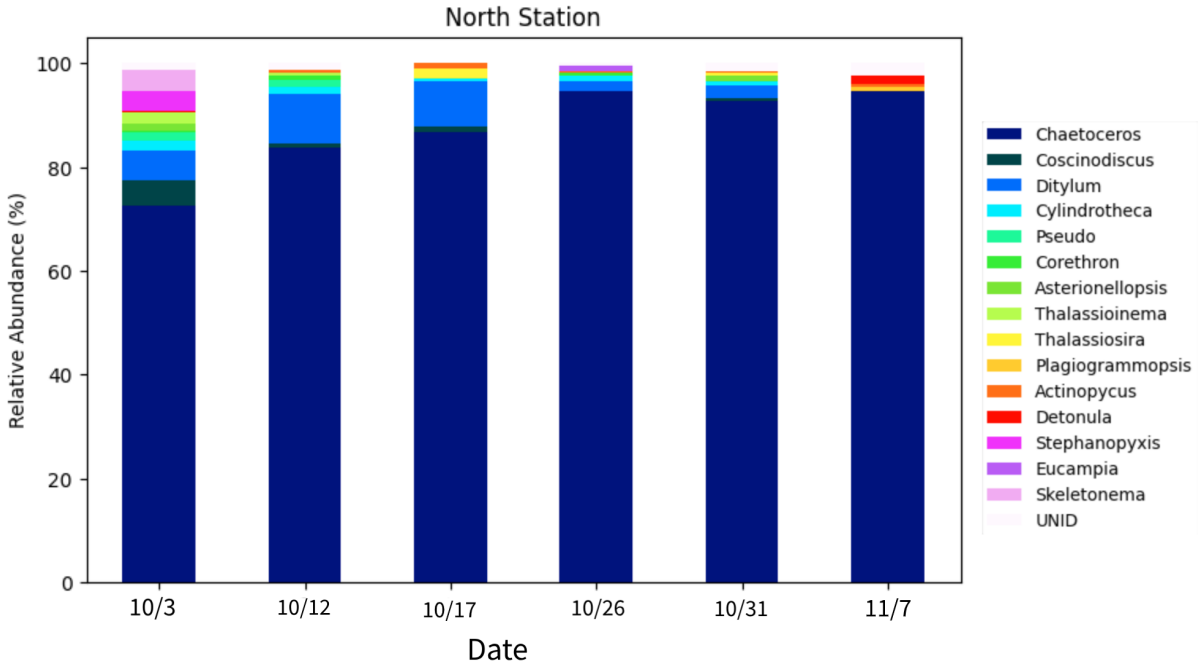

Figure 7. Fall 2023 Time series of the relative abundance of all genera found at North

Fig. 8

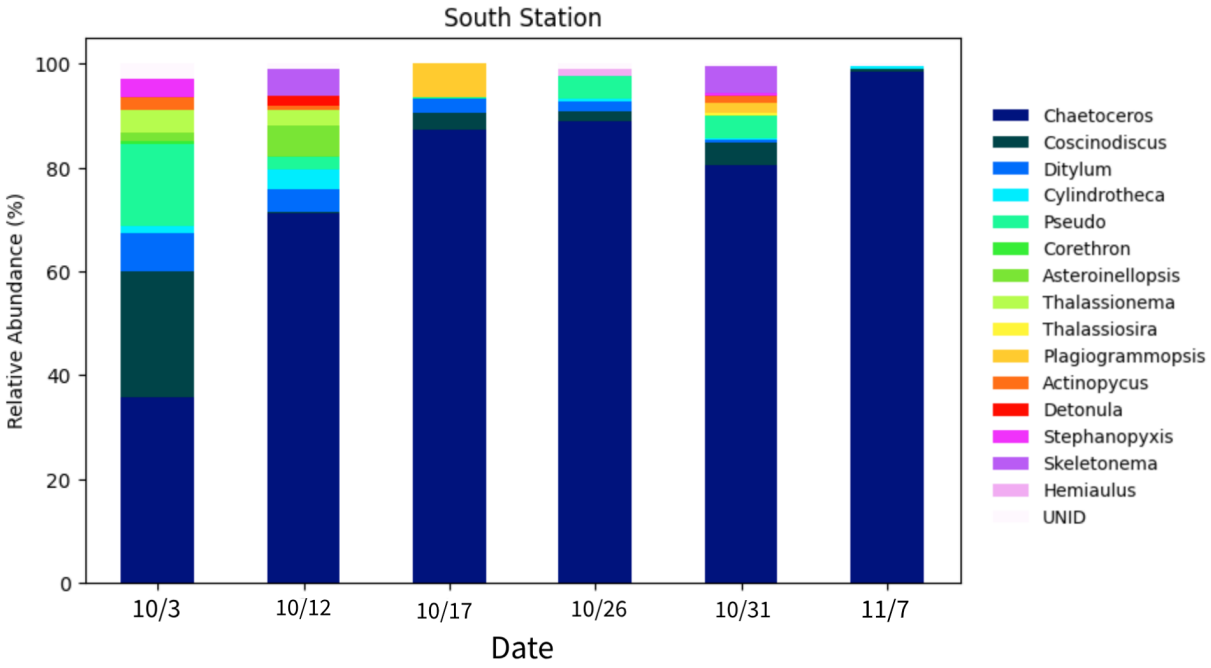

Figure 8. Time series of the relative abundance of all genera found at South

Fig. 9

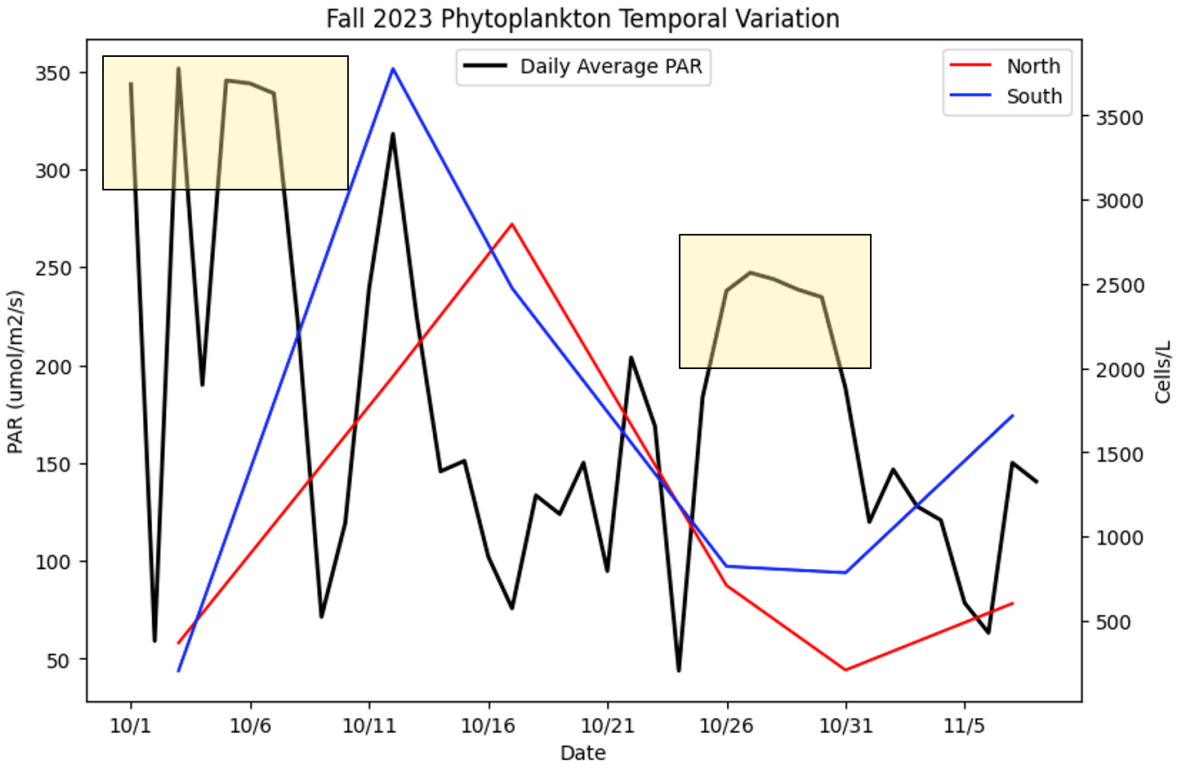

Figure 9. Daily average PAR with abundance at each station. Periods of sunny days are highlighted in yellow. PAR data via FHL Weather Station (http://wx.fhl.washington.edu/vdv/VV_Frame.php)

Fig. 10

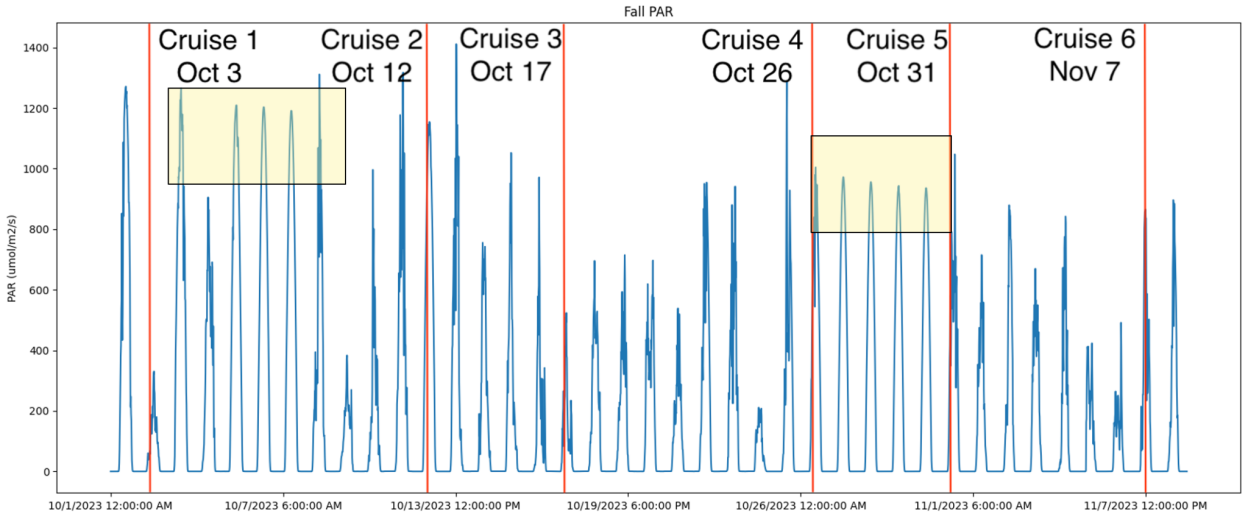

Figure 10. Time series of PAR from October 1st to November 8th 2023. Cruises are marked with a vertical red line and labeled. Periods of sunny days are highlighted in yellow.

Fig. 11

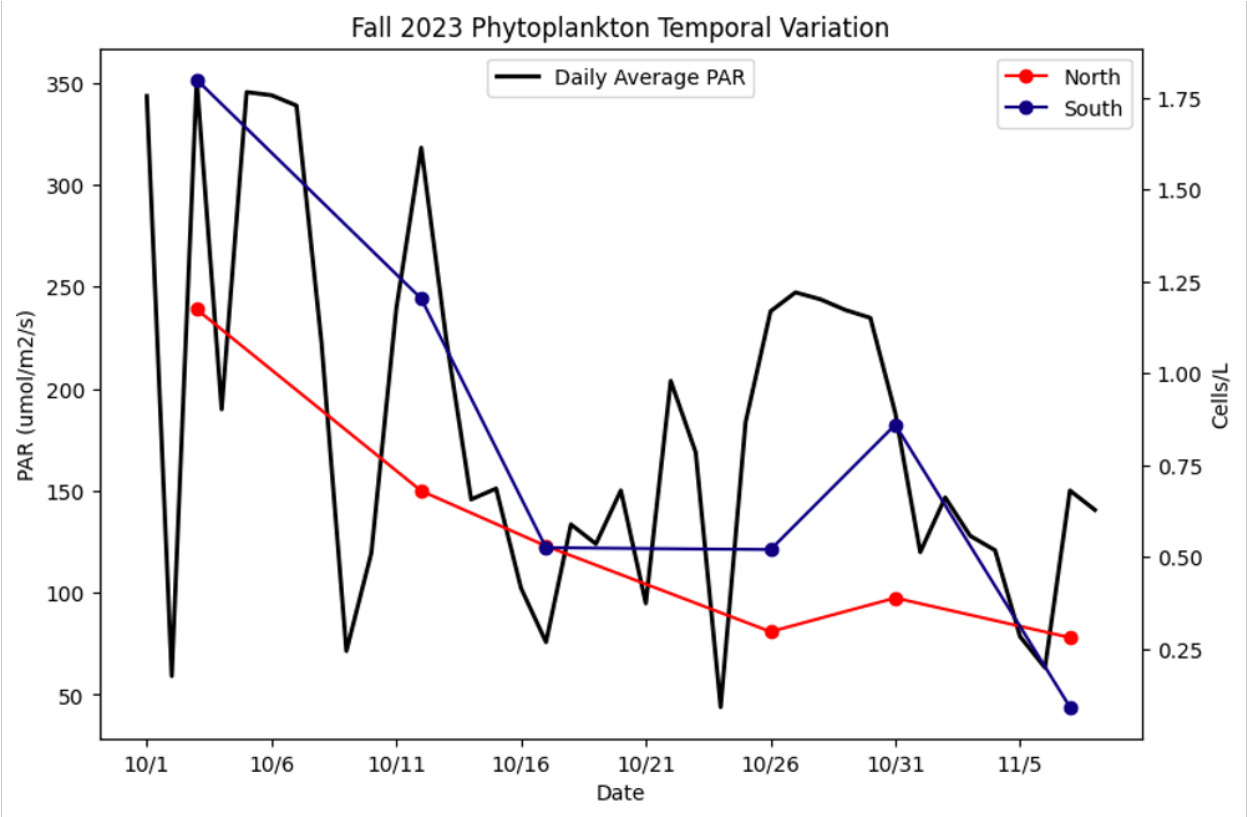

Figure 11. Daily average PAR with diversity at each station.

Fig. 12

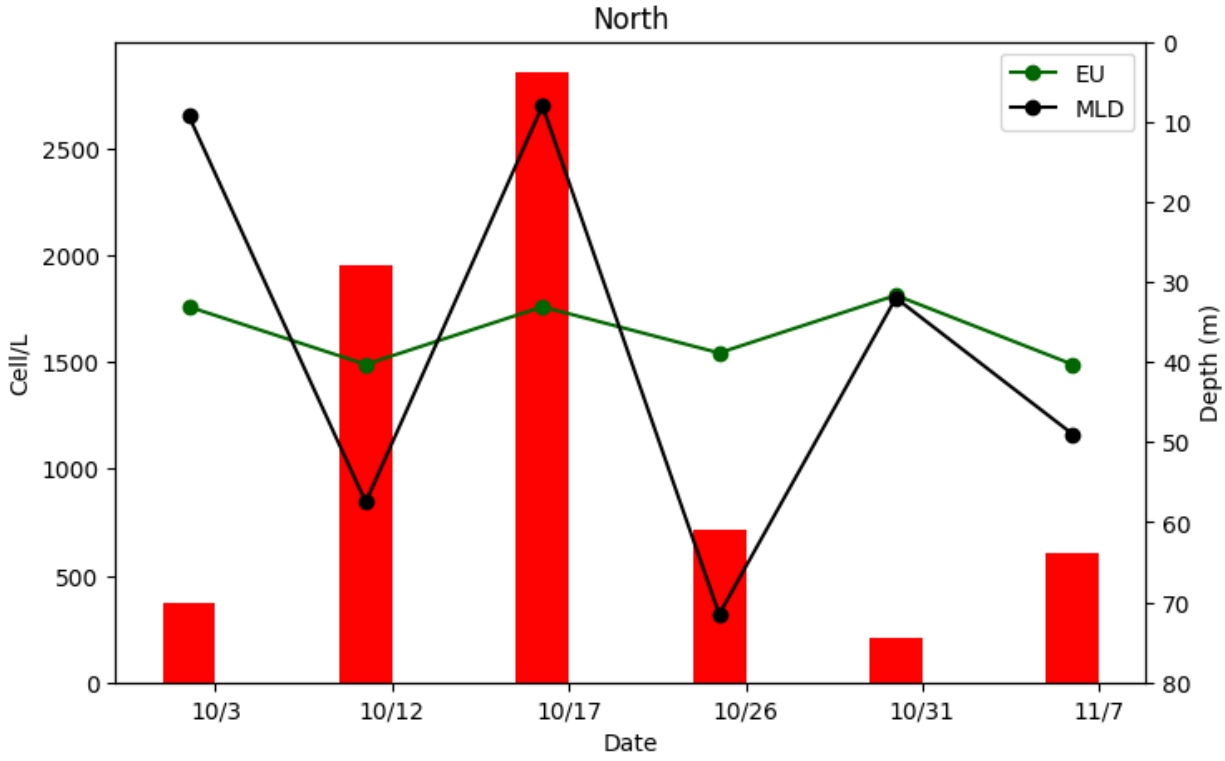

Figure 12. Time series of phytoplankton abundance with the depth of the mixed layer and euphotic zone at Station North.

Fig. 13

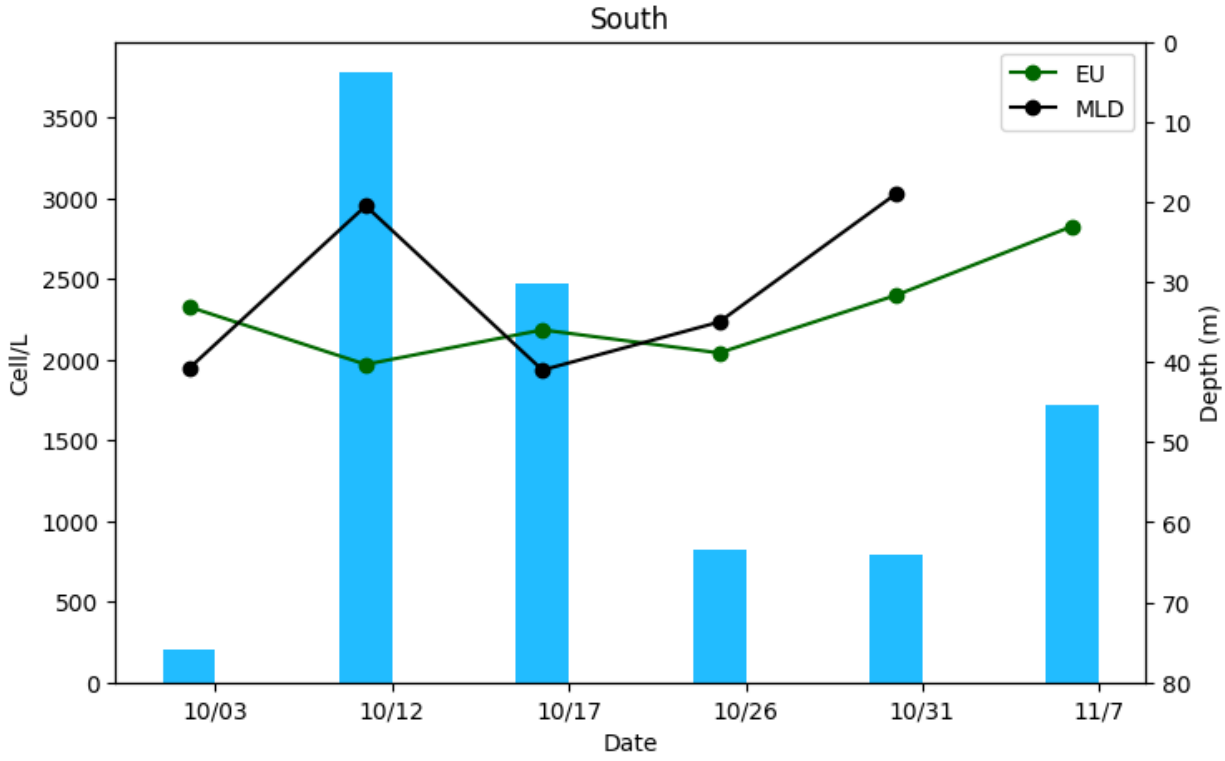

Figure 13. Time series of phytoplankton abundance with the depth of the mixed layer and euphotic zone at Station South.

Fig. 14

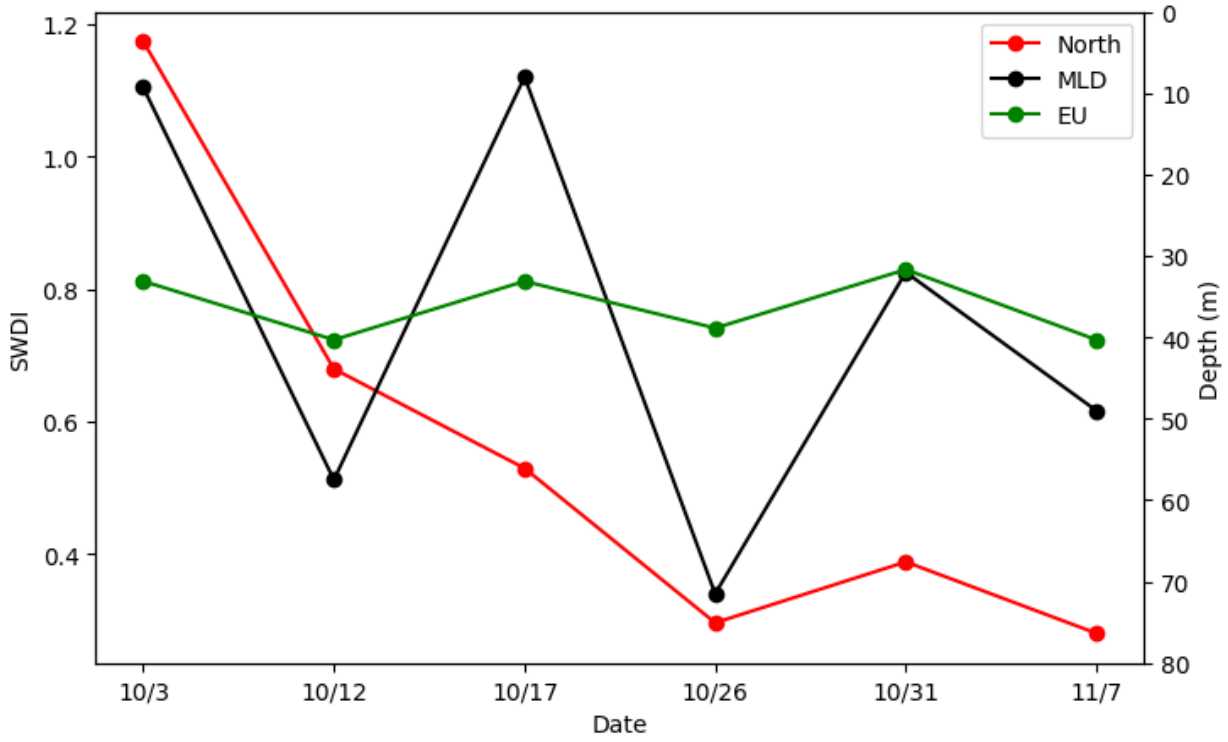

Figure 14. Time series of phytoplankton diversity with the depth of the mixed layer and euphotic zone at Station North.

Fig. 15

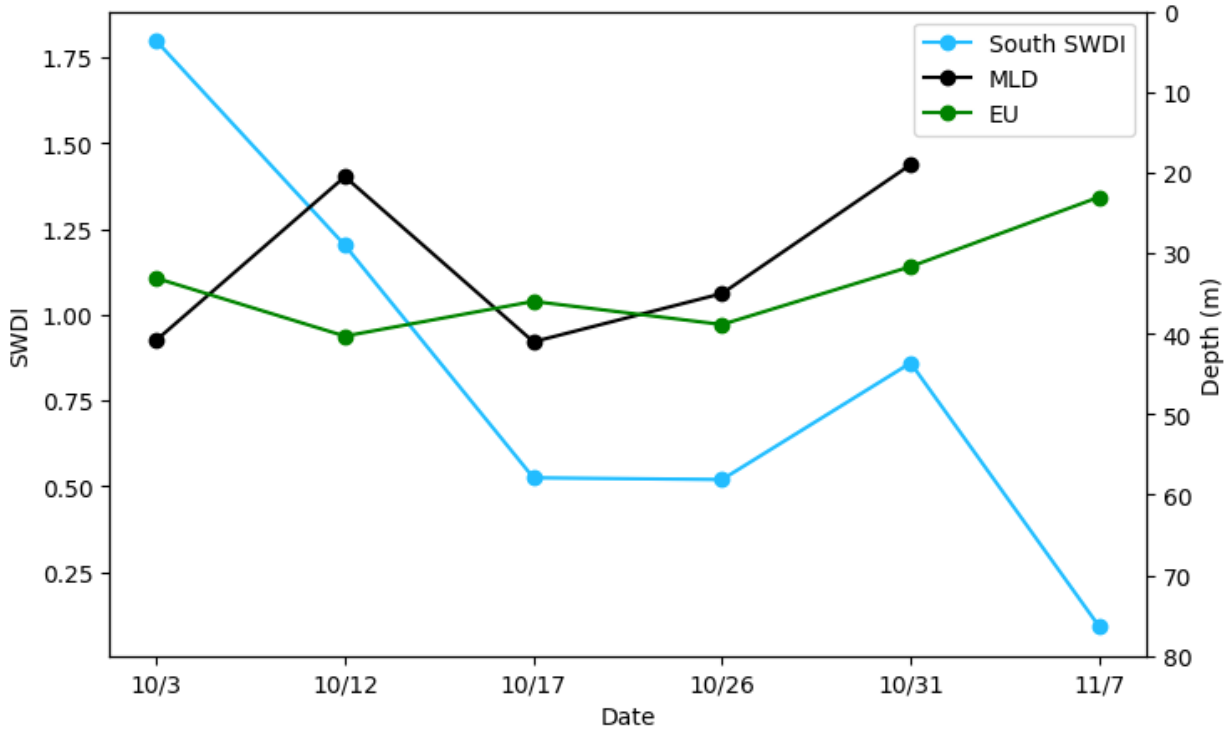

Figure 15. Time series of phytoplankton diversity with the depth of the mixed layer and euphotic zone at Station South.